INTERNATIONAL JOURNAL FOR NUMERICAL METHODS IN FLUIDS
Int. J. Numer. Meth. Fluids 2008; **56**:1281–1287
Published online 5 December 2007 in Wiley InterScience (www.interscience.wiley.com). DOI: 10.1002/fld.1671

Simulation of high-speed flows by an unstructured grid implicit method including real gas effects

M. Y. Hashemi and A. Jahangirian*, †

Center of Excellence in Computational Aerospace and Department of Aerospace Engineering, Amirkabir University of Technology, Tehran, Iran

SUMMARY

The incorporation of real gas effects into an efficient dual-time implicit method is presented for numerical simulation of high-speed flows. Two-dimensional compressible Navier–Stokes equations are discretized by an implicit approach in a real-time basis. The resulting set of implicit nonlinear equations is then solved iteratively in pseudo-time using a Runge–Kutta scheme. A control-volume central difference approach is used for spatial discretization on unstructured grids. For an equilibrium chemically reacting air, simplified equations are used to calculate the thermodynamics and transport properties of equilibrium air. The method is applied to hypersonic laminar flows of air over a compression ramp and a circular cylinder. Computational results are compared with those of other numerical methods and experimental data. Excellent agreement is obtained for various flow and heat transfer characteristics. Considerable reduction in computational time has also been achieved compared with the original explicit method. Copyright © 2007 John Wiley & Sons, Ltd.

Received 27 April 2007; Revised 11 October 2007; Accepted 12 October 2007

KEY WORDS: real gas; high-speed flow; implicit dual-time stepping; unstructured grid

1. INTRODUCTION

Recent advances in computing power has attracted much attention to the development of computational fluid dynamics (CFD) methods particularly for high-speed flow applications. CFD is expected to play a major role in the simulation of high-speed flight because of the difficulties involved in producing data from experimental facilities [1]. On the other hand the main considerations for CFD methods are accurate simulation of flows with strong shock waves, capturing complex flow phenomena and variation of flow variables at high-speed conditions. Several researches have been conducted in order to introduce modifications to the existing numerical methods for application in

*Correspondence to: A. Jahangirian, Department of Aerospace Engineering, Amirkabir University of Technology, Tehran, Iran.
†E-mail: ajahan@aut.ac.ir

hypersonic flow problems [2–4]. However, certain numerical problems may still arise including the spurious non-physical oscillations in the vicinity of strong shock waves, errors in the conservation of total temperature as well as the development of accurate thermodynamic models to include real gas effects. One of the other major problems encountered in the numerical solution of hypersonic flows is the slow rate of convergence. In high-speed flows, small Courant–Friedrichs–Lewy (CFL) numbers are usually dictated by stability requirements of explicit numerical algorithms. Several attempts have therefore been carried out for presenting efficient and robust implicit methods applicable to hypersonic flows [5]. However, the incorporation of real gas effects is only considered in few works. The dual-time implicit method presented by Jameson [6] has proven to be an efficient method for steady and unsteady calculations on structured [6] and unstructured grids [7] in transonic flows. In the present work, the extension of this method to hypersonic flows including real gas effects is investigated on unstructured grids.

2. MATHEMATICAL MODEL

2.1. Governing flow equations

Two-dimensional compressible viscous flow is governed by a conservative form of Navier–Stokes equations in the Cartesian coordinate system as

$$\frac{\partial \omega}{\partial t}+\frac{\partial (f^I)}{\partial x}+\frac{\partial (g^I)}{\partial y}=\frac{\partial (f^V)}{\partial x}+\frac{\partial (g^V)}{\partial y} \tag{1}$$

where ω is the vector of conserved flow variables, f^I and g^I represent the convective fluxes and f^V, g^V define the viscous diffusion terms. Applying Equation (1) to each cell in the computational domain, the result will be a set of ordinary differential equations in the following form:

$$A_k \frac{\partial}{\partial t}(\omega_k)+R_k(\omega)-D_k(\omega)=0 \tag{2}$$

where A_k is the cell area and $R_k(\omega)$ contains the convective and viscous fluxes. The properties over each cell edges are evaluated using an averaging method [8]. The artificial dissipation fluxes $D_k(\omega)$ are also added in order to prevent the oscillations particularly in the neighborhood of shock waves. A blend of second and fourth differences with coefficients that depend on local pressure gradients is used in the present work. More details about the development of these terms can be found in [8].

2.2. Implicit time integration

The $\partial/\partial t$ operator in Equation (2) can be approximated by an implicit backward difference formula of kth order of accuracy. Using a second-order accurate time discretization, Equation (2) can be expressed in a fully implicit form (in real time) [7] as

$$A_k\left(\frac{3}{2\Delta t}(\omega_k^{n+1})-\frac{2}{\Delta t}(\omega_k^n)+\frac{1}{2\Delta t}(\omega_k^{n-1})\right)+R_k(\omega^{n+1})-D_k(\omega^{n+1})=0 \tag{3}$$

At this stage it is convenient to redefine a new residual R^*, referred to as unsteady residual, which is equal to the left-hand side of Equation (3). The new equation can be seen as the solution of

DOI: 10.1002/fld

a steady-state problem which can then be solved with a time marching method by introducing a derivative with respect to a fictitious pseudo-time τ:

$$A_k \frac{\partial}{\partial \tau}(\omega_k^{n+1}) + R_k^*(\omega^{n+1}) = 0 \tag{4}$$

Equation (4) is the modified steady-state problem in pseudo-time. This problem can be solved by using the explicit Runge–Kutta multistage scheme. To accelerate convergence, local pseudo-time stepping and implicit residual averaging are used in the present work [7].

In the far field, non-reflecting boundary conditions are used based on the characteristic analysis or Newmann boundary condition. At the solid wall boundary, the components of velocity vector are set equal to zero. The value of the pressure at the solid wall can be obtained by extrapolating from the values of the adjacent cell centers.

3. INCORPORATION OF REAL GAS EFFECTS

In the hypersonic flows, the temperature inside the boundary layer and behind the shock wave is so high that chemical reactions can occur. The chemical reactions cause varying physical properties of the air such as thermal conductivity K, specific heat ratio γ and the coefficient of viscosity μ. In this condition the air cannot be assumed a perfect gas since the assumption of constant γ can lead to over-prediction of temperature and pressure near stagnation conditions. Real gas effects for compressible flow calculations have been presented by many researchers using reaction equations for calculating K, μ and γ [9] or using the simplified curve fits to obtain the thermodynamics and transport properties of equilibrium air [10, 11]. In the present work, the incorporation of the real gas model is implemented by using a generalized equation of state, introducing an equivalent ratio of specific heat $\widetilde{\gamma}$. The equations for thermodynamics and transport properties are used from the work of Srinivasan and co-workers [10, 11] in the form

$$\widetilde{\gamma} = \widetilde{\gamma}(e, \rho), \quad P = \rho e(\widetilde{\gamma} - 1), \quad T = T(P, \rho), \quad \mu = \mu(T, \rho), \quad K = K(e, \rho) \tag{5}$$

The above equations are implemented every fifth iteration in the explicit loops in order to update the variables. The numerical experiments showed that this process does not affect the stability and accuracy of the solution while saving the computational time.

4. NUMERICAL RESULTS

Validation of the proposed method for hypersonic flows has been carried out using two well-known test cases i.e. a compression ramp and a blunt body.

4.1. Compression corner

For the first geometry, two test cases are considered. The first case is the case number 3.4 of the workshop on hypersonic flows [12]. The flow conditions contain the free stream temperature of 65 K, Mach number of 11.68, wall temperature of 289.95 K and the Reynolds number of 247 000. The experimental data for this case may be obtained from Holden [13]. In this case, the grid study has been implemented using three computational grids including 4800, 8400 and 13 000

DOI: 10.1002/fld

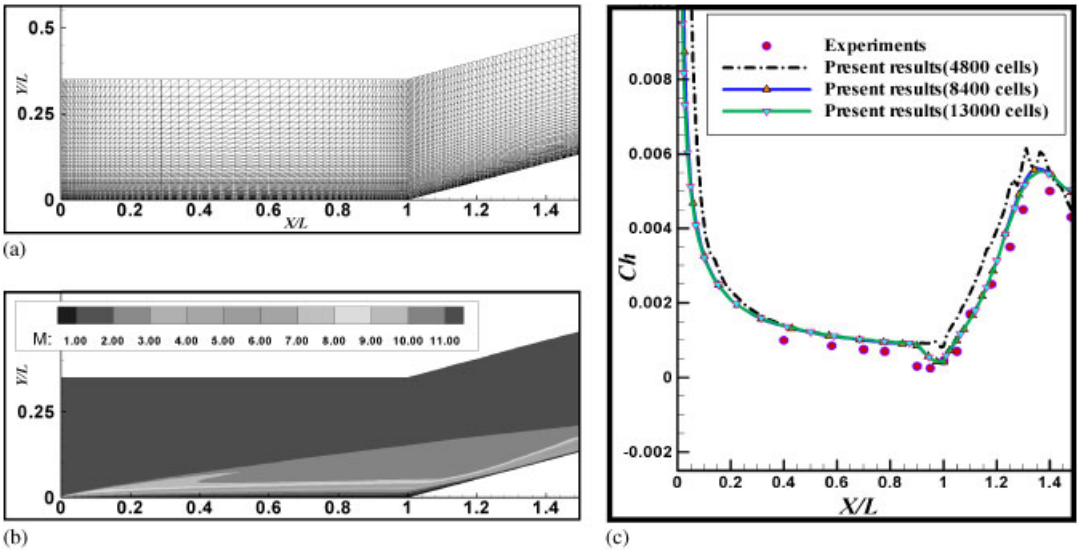

Figure 1. (a) Computational grid; (b) Mach number contours; and (c) heat transfer coefficient along the surface for the ramp in Mach number 11.68.

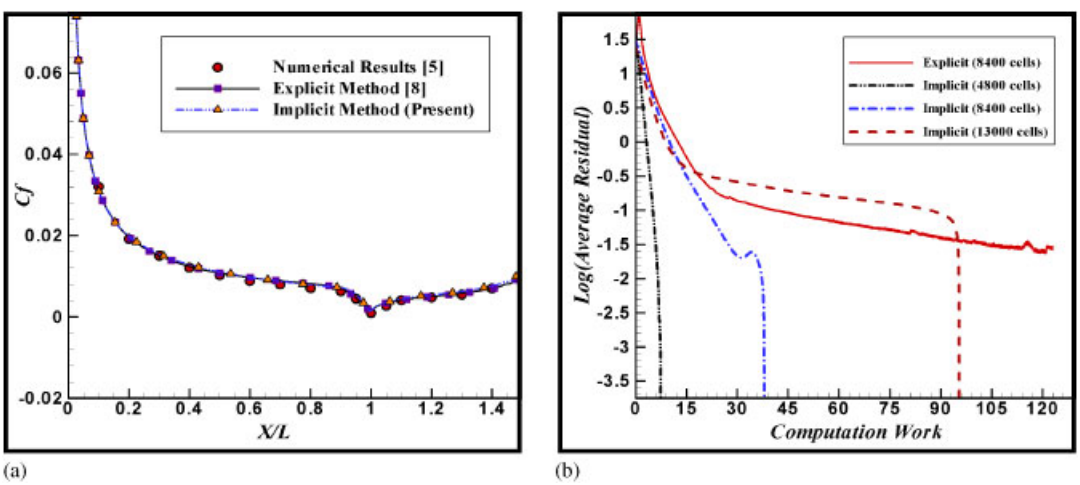

Figure 2. (a) Friction factor and (b) convergence history for the ramp in Mach number 10.

cells regarded as coarse, medium and fine grids, respectively. Figure 1(a) shows the medium grid that has 105 points along the surface and 40 points in the normal direction. The Mach number contours within the domain are shown in Figure 1(b). Figure 1(c) illustrates the surface heat transfer coefficient obtained from the present numerical method for three different grids compared with the experimental data [13]. It is evident from this figure that the coarse grid results are not accurate particularly near shock wave interaction positions. However, no significant difference can be recognized between the medium and fine grid results. Therefore, the medium grid is chosen

DOI: 10.1002/fld

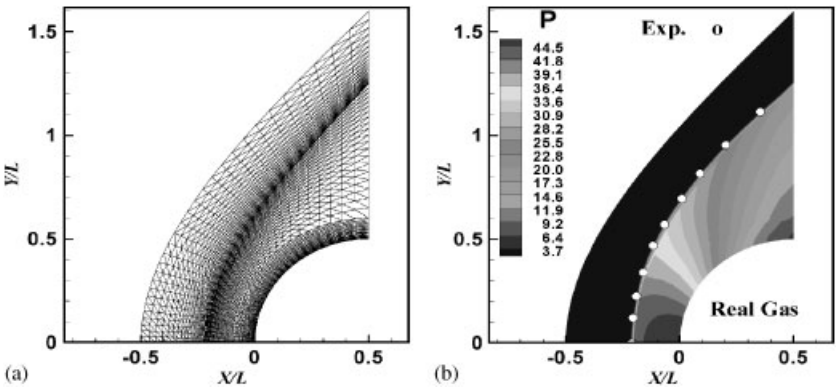

Figure 3. Flow around circular cylinder; $M_\infty = 6$: (a) computation grid and (b) pressure contours.

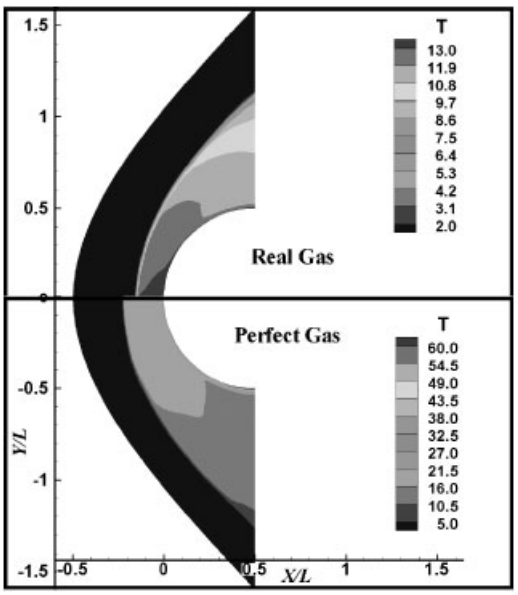

Figure 4. Temperature ratio contours for perfect gas and real gas calculations, $M_\infty = 10$.

for calculations in this case with real time step (CFL) of 50 000 and pseudo-time step of 2.5. A second set of flow conditions for this geometry is chosen as $M_\infty = 10$, $Re_\infty = 18\,000$, $T_\infty = 52\,\mathrm{K}$ and $T_{\mathrm{wall}} = 289.95\,\mathrm{K}$ in order to compare the current results with the numerical results of [5] and the original explicit method [8]. Figure 2(a) shows the friction factor distribution along the surface for the above three methods. As illustrated, good agreement is evident in this figure between three numerical results. The convergence behavior of the presented implicit method is compared with that of the original explicit method [8] in Figure 2(b) against the computational time. The implicit results are presented for three different grids i.e. fine, medium and coarse grids as introduced above. It is shown that the implicit method has remarkable computational efficiency compared with

DOI: 10.1002/fld

the explicit one. As expected, the coarse grid presents faster convergence; however, as discussed before the accuracy of the results with this grid is not satisfactory.

4.2. Circular cylinder

The second geometry is a circular cylinder at free stream conditions of $M=6, T=225\,\mathrm{K}$ and $P=48.76\,\mathrm{Pa}$ corresponding to the atmospheric conditions at an altitude of 52 km. The wall of cylinder is considered adiabatic. The generated grid for this case is shown in Figure 3(a) containing 6600 grid cells. The real-time CFL number of 100 000 with the pseudo-time CFL number of 2.5 are utilized in this case. Figure 3(b) shows the location of the shock wave obtained from the experimental data [14] compared with that of the present numerical method taken from the pressure contours. As illustrated, the shock position is well predicted by the present method. Finally, in order to show the effect of real gas model incorporation the iso-temperature ratio lines are compared in Figure 4 for free stream Mach number of 10. As expected, the perfect gas results contain much higher temperatures behind the shock wave compared with the real gas one.

5. CONCLUSIONS

The incorporation of real gas effects into an unstructured grid dual-time implicit method was presented for hypersonic laminar flows of air over a compression ramp and a circular cylinder. For an equilibrium chemically reacting air, simplified equations were used to calculate the thermodynamics and transport properties of equilibrium air. Excellent agreement has been obtained for various flow and heat transfer characteristics. Considerable reduction in computational time has also been achieved compared with the original explicit method.

REFERENCES

1. Johnston IA. Simulation of flow around hypersonic blunt-nosed vehicles for the calibration of air data systems. *Ph.D. Thesis*, The University of Queensland, Australia, January 1999.
2. Drikakis D, Tsangaris S. On the accuracy and efficiency of CFD methods in real gas hypersonic. *International Journal for Numerical Methods in Fluids* 1993; **16**:759–775.
3. Coirier WJ. Efficient real gas upwinded Navier–Stokes computation of high speed flows. *AIAA Journal* 1991; **29**(8):1223–1231.
4. Tannehill JC, Levalts JO. An upwind parabolized Navier–Stokes code for real gas flows. *AIAA-1988-713*, *Aerospace Sciences Meeting*, *26th*, Reno, NV, 11–14 January 1988.
5. Thomas JL. An implicit multi-grid scheme for hypersonic strong-interaction flow fields. *Communications in Applied Numerical Methods* 1992; **8**:683–693.
6. Jameson A. Time dependent calculations using multi-grid with applications to unsteady flows past airfoils and wings. *AIAA-1991-1596*, *CFD Conference*, *10th*, Honolulu, HI, 24–26 June 1991.
7. Jahangirian A, Hadidoolabi M. Unstructured moving grids for implicit calculation of unsteady compressible viscous flows. *International Journal for Numerical Methods in Fluids* 2005; **47**:1107–1113.
8. Mavriplis DJ, Jameson A. Multi-grid solution of the Navier–Stokes equations on triangular meshes. *AIAA Journal* 1990; **28**(8):1415–1425.
9. Wood WA, Eberhardt S. Dual-code solution strategy for chemically-reaction hypersonic flows. *AIAA-1995-158*, *Aerospace Sciences Meeting and Exhibit*, *33rd*, Reno, NV, 9–12 January 1995.
10. Srinivasan S, Tannehill JC. Simplified curve fits for the transport properties of equilibrium air. *NASA CR-178411*, December 1987.
11. Srinivasan S, Tannehill JC, Weilmuenster KJ. Simplified curve fits for the thermodynamic properties of equilibrium air. *NASA RP-1181*, 1987.

DOI: 10.1002/fld

12. Rudy DH, Thomas JL, Kumar A, Gnoffo PA, Chakravarthy SR. Computational study of laminar hypersonic flow over a 2-D ramp. *Workshop on Hypersonic Flows for Reentry Problems*, Antibes, France, Part 2, 1991.
13. Holden MS. A study of flow separation in regions of shock-wave boundary layer interaction in hypersonic flow. *AIAA Paper 78-1169*, 1978.
14. Billig FS. Shock-wave shapes around spherical and cylindrical-nosed bodies. *Journal of Spacecraft* 1967; **4**(6):822–823.

DOI: 10.1002/fld